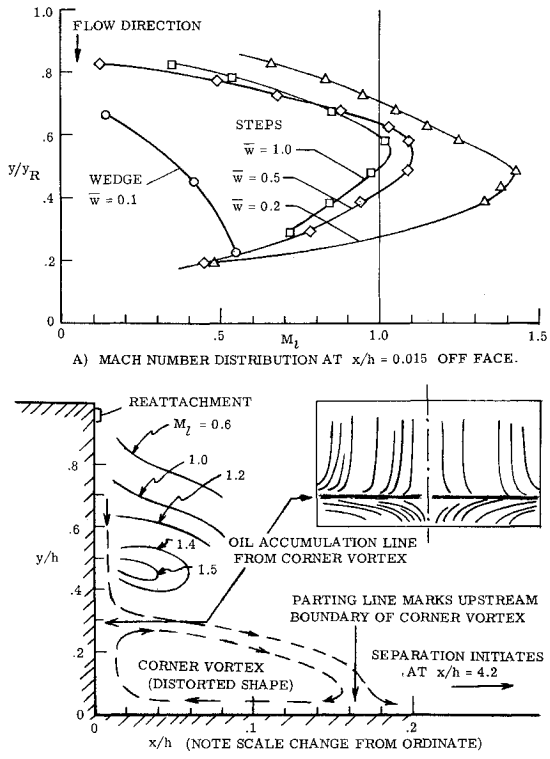

Fig. 3 Mach number distribution down faces of wedges and steps. $M_\infty = 6.0$; $R/m = 21 \times 10^6$.

Oil flow results from the $\bar{w} = 0.2$ step face shown in Fig. 3b (obtained from a tracing of the photograph) identified a local vortex flow in the bottom corner of the step. The flow up the face from the corner is then opposed by the flow moving down the face from reattachment, resulting in an oil accumulation line located near $y/h = 0.3$ for the $\bar{w} = 0.2$ step. This secondary vortex was observed in the corners of all steps in this investigation and also in the tests reported by Behrens.[5] Mach number contours obtained from probe surveys at stations off the $\bar{w} = 0.2$ step face are sketched in Fig. 3b (note that the horizontal and vertical scales are dissimilar). A considerable portion of this flow down the face is found to be supersonic. A shock system is probably required in the neighborhood of the oil accumulation line to decelerate the flow as it approaches the corner.

The present study has shown the critical importance of transverse outflow in determining some of the characteristic features of a turbulent, separated boundary layer. Continued refinements in two-dimensional analytical methods which do not account for transverse-outflow effects are of limited benefit to the designer of hypersonic vehicles who must be concerned with finite-span separations. Mach number profiles when considered with oil flow patterns permit an elementary modeling of the reverse flow region adjacent to the face of a forward-facing step with transverse outflow.

References

[1] Roshko, A., "Review of Concepts in Separated Flow," *Canadian Congress of Applied Mechanics*, edited by B. H. Karnopp of Toronto, Vol. 3, May 1967, pp. 3–81 to 3–115.

[2] Chapman, D. R., Kuehn, D. M., and Larson, H. K., "Investigation of Separated Flows in Supersonic and Subsonic Streams With Emphasis on the Effects of Transition," Rept. 1356, 1958, NACA.

[3] Hefner, J. N., and Whitehead, A. H. Jr., "Lee-Side Heating Investigations: Part I—Experimental Lee-Side Heating Studies on a Delta-Wing Orbiter," TM X-2272, March 1971, NASA.

[4] Morrisette, E. L., Stone, D. R., and Whitehead, A. H., Jr., "Viscous Drag Reduction," *Boundary Layer Tripping With Emphasis on Hypersonic Flows*, edited by C. S. Wells, Plenum Press, N.Y., pp. 33–51.

[5] Behrens, W., "Separation of a Supersonic Turbulent Boundary Layer by a Forward Facing Step," AIAA Paper 71–127, New York, 1971.

[6] Sterrett, J. R. and Barber, J. B., "A Theoretical and Experimental Investigation of Secondary Jets in a Mach 6 Free Stream With Emphasis on the Structure of the Jet Separation Ahead of the Jet," *Proceedings of the Agard Conference 4, Separated Flows, Part II*, May 1966, pp. 667–700.

[7] Zukoski, E. E., "Turbulent Boundary-Layer Separation in Front of a Forward-Facing Step," AIAA Journal, Vol. 5, No. 10, Oct. 1967, pp. 1746–1753.

[8] Sterrett, J. R. and Emery, J. C., "Extension of Boundary-Layer-Separation Criteria to a Mach Number of 6.5 by Utilizing Flat Plates With Forward-Facing Steps," TN D-618, Dec. 1960, NASA.

Impact Probe Displacement in a Supersonic Turbulent Boundary Layer

JERRY M. ALLEN*
NASA Langley Research Center, Hampton, Va.

Nomenclature

D = impact probe outside diameter
M = Mach number
M_e = boundary-layer edge Mach number
Y = distance normal to test surface
δ = boundary-layer thickness
Δ = impact probe displacement

1. Introduction

IMPACT pressure measurements in boundary-layer research are usually performed with probes which are very small relative to the boundary-layer thickness in order to minimize any influences of probe size on the resulting measurements. When this is not possible, and the experimenter wants to correct his measurements for probe displacement effects, the works of Young and Maas[1] and MacMillan[2] are available for incompressible wakes and incompressible turbulent boundary layers, respectively. A literature search, however, revealed that no comparable work has been performed in a supersonic turbulent boundary layer. The bow shock wave ahead of an impact probe in supersonic flow could significantly affect the displacement compared to the incompressible case. This study was thus undertaken to provide experimental impact probe displacement results in a two-dimensional supersonic turbulent boundary layer.

2. Experiment

The experiment was performed on the test section sidewall in Langley's 4-ft × 4-ft supersonic pressure tunnel.[3] The nominal freestream Mach number of 2.0, stagnation pressure of 0.69 atm, and stagnation temperature of 41°C resulted in a unit Reynolds number of about 8×10^6/m and a Reynolds number based on the distance from the tunnel throat to the survey station of about 43×10^6.

The boundary layer at the test station was surveyed in turn by each of 8 impact probes ranging in size from about 1.3 to 48 mm. This largest probe was about 70% of the boundary-layer thickness. The probes were circular in cross section and had inside-to-outside diameter ratios of about 0.6. The impact pressures measured by these probes were combined with the test section static pressure to calculate Mach numbers. Probe displacement effects were evaluated in terms of these Mach number values.

3. Discussion

Figure 1 shows the probe Mach number variations with probe diameter. The curves connect points of constant Y; that is, points whose probe centers are located at the same position in the boundary layer. The extrapolation of these curves to $D = 0$ should give the true Mach number profile for this boundary layer.

Received November 19, 1971.

* Aerospace-Technologist, High-Speed Aircraft Division. Member AIAA.

The solid symbols indicate points where the probe was touching the wall.

At the smaller diameters there appears to be a linear increase in Mach number with probe diameter. The measured Mach number being larger than the true Mach number is termed positive displacement.

Proceeding from left to right along any one curve in this figure results in the probe coming into closer proximity to the wall since the centers of the probes remain at the same location and the diameters increase. This wall influence region causes the displacement to decrease at the larger probe diameters. The point at which deviation from the linear curve begins is at Y/D values of about 1; that is, the wall influence region extends to about one probe diameter away from the wall. Note that the Mach numbers measured at the wall contact points (solid symbols) are very close to the true Mach number at that value of Y. This indicates that probe displacement effects in Preston tube work are probably negligible.

The kinks in the curves in the upper right in this figure result from distortion of the boundary layer by the larger probes. (Data for Y/δ values larger than 0.782 were omitted from this figure for clarity.) Note that some of the indicated Mach numbers are larger than the boundary layer edge value; referred to hereafter as Mach number overshoot. This distortion pattern can be seen more clearly in Fig. 2, where the measured and true Mach number profiles are compared.

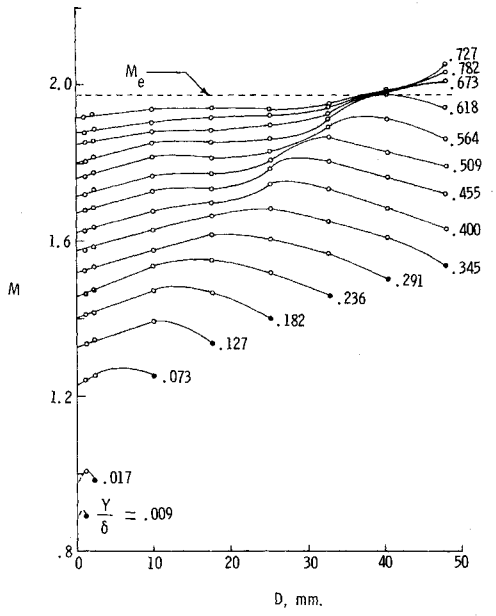

Fig. 1 Effect of probe size on measured Mach numbers.

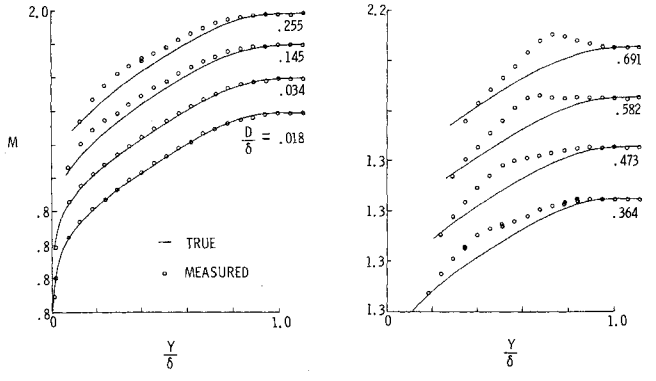

Fig. 2 Comparison of true and measured profiles.

The profiles for the two smallest diameter probes appear normal, but show positive displacement. The $D/\delta = 0.145$ profile contains a small region of distortion near the wall. This region spreads and becomes more pronounced with increasing probe size. Profiles from the two largest probes have the regions of Mach number overshoot mentioned previously.

The displacement effect of these probes is the distance that the measured data are displaced from the true profile; that is, the horizontal distance between the curve and symbols in this figure. These displacement distances were measured for each data point and are shown in Fig. 3.

The displacement for the smaller probes appears within the accuracy of the data to be constant over most of the boundary layer. For small Y/δ values, the displacement decreases to near zero because of the wall effect mentioned previously. The relatively large scatter in the data near the boundary-layer edge is caused by the small Mach number gradients in this region, making accurate displacement measurements impossible. The displacement levels were thus faired to zero at $Y/\delta = 1$ since there should be no probe displacement in the freestream.

The distortion regions appear as peaks in the displacement curves. Beyond these distortion regions, however, there are still regions for the moderate diameter probes where the displacement remains constant before dropping to zero in the freestream. For the $D/\delta = 0.473$ probe, the distortion covers most of the boundary layer, leaving no room for the constant-displacement region. The probes with Mach number overshoot show regions of infinite displacement.

The previous experiments in incompressible flow[1,2] have shown that the ratio of displacement to probe diameter is independent of probe diameter in the absence of wall effects. Hence the constant-level values of displacement were ratioed to the respective probe diameter and are shown in Fig. 4 as a function of probe diameter.

The $D = 0$ point in this figure was estimated from the slopes of the lines in Fig. 1 ($\partial M/\partial D$) and the slopes of the true Mach number profile ($\partial M/\partial Y$). As D approaches zero it can be shown that Δ/D approaches $(\partial M/\partial D)/(\partial M/\partial Y)$. Values of Δ/D were calculated for each Y value and averaged to give the point shown in this figure.

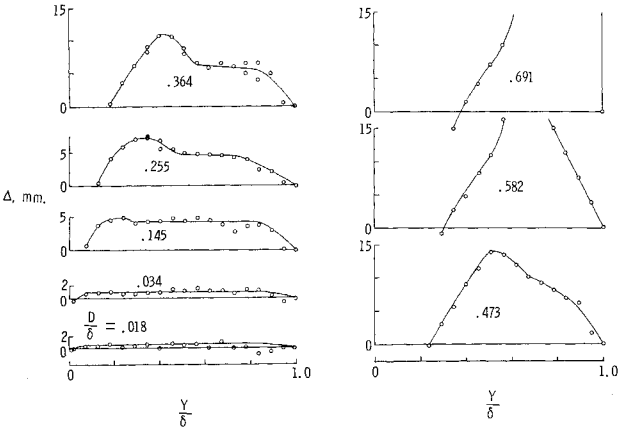

Fig. 3 Impact probe displacement distributions.

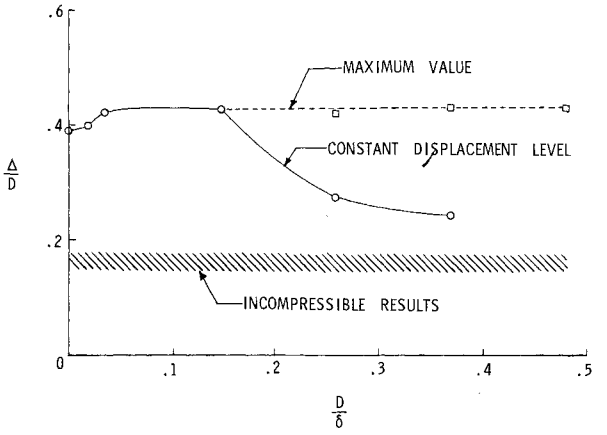

Fig. 4 Effect of probe size on displacement ratio.

This limiting point agrees well with the values from the distortion-free probes. The larger probes, however, show decreasing values in the constant-displacement regions. It is interesting to note that if the maximum values of Δ/D are plotted instead of the constant-displacement values, the agreement with the smaller diameter data is good.

Included on this figure for comparison is the level of Δ/D obtained by previous investigations[1,2] in incompressible flow. The displacement level obtained in this study is more than double that obtained previously in incompressible flow.

References

[1] Young, A. D. and Maas, J. N., "The Behavior of a Pitot Tube in a Traverse Total-Pressure Gradient," R and M 1770, Sept. 1936, Aeronautical Research Council.

[2] MacMillan, F. A., "Experiments on Pitot-Tubes in Shear Flow," R and M 3028, Feb. 1956, Aeronautical Research Council, National Physical Lab., Teddington, England.

[3] Schaefer, William T. Jr., "Characteristics of Major Active Wind Tunnels at the Langley Research Center," TM X-1130, July 1965, NASA.

Further Experimental Studies of Cross-Hatching

HANS W. STOCK* AND JEAN J. GINOUX†
von Kármán Institute for Fluid Dynamics, Rhode-Saint-Genèse, Belgium

A CONCLUSIVE theoretical explanation of the phenomenon of cross-hatching is still outstanding,[1-3] and consequently, additional experimental observations are of interest.

This Note describes the effect of nose blunting, exposure time and initial temperature of axisymmetric bodies on the main characteristics of the ablation surface pattern. The study was made in the same facility, under similar stagnation conditions, as in Ref. 4. Cones of 10–62° total vertex angle were tested at zero angle of attack. The ablation materials were wax and camphor, which liquefied and sublimed respectively under the present test conditions.

1. Effect of Nose Blunting

Figure 1 shows the cant angle ϕ of crosshatched patterns observed on self-blunting cones, consisting entirely of ablation material, vs Mach number M_e, where M_e is calculated for sharp nose cones. These results are compared with those previously obtained on sharp nose models which followed the Mach angle trend, shown by the solid curve. Present data agree with free-flight results[5] and thus prove that the apparent "freezing" of ϕ for Mach numbers M_e larger than 3 is due to nose blunting, i.e. improper use of M_e instead of the actual local Mach number on the blunt nose cones.

2. Effect of Exposure Time

There was for each test conditions an optimum wind-tunnel running time t after which a well contrasted pattern was observable. A typical run time on a 26° total angle cone was 15 sec ± 2 sec. The pattern is nonexistent or too weak for a run time less than 13 sec and disorganized for times larger than 17 sec.

Figure 2 shows this time t as a function of the static pressure p_e, for a nearly constant temperature ratio $(T_r - T_W)/T_W = 0.0989 - 0.1278$. The recovery temperature T_r was calculated by assuming

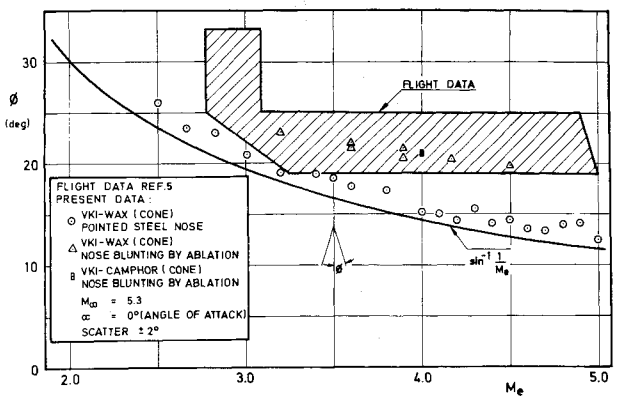

Fig. 1 Influence of the Mach number M_e on the cant angle $\phi = M_e$ calculated for unblunted cones.

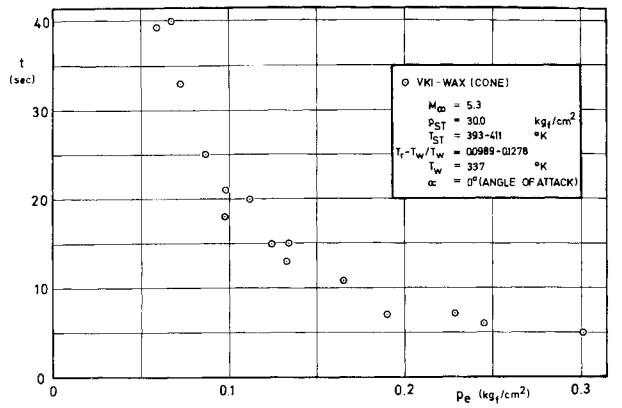

Fig. 2 Run time required for a developed cross-hatched pattern as a function of the local static pressure p_e.

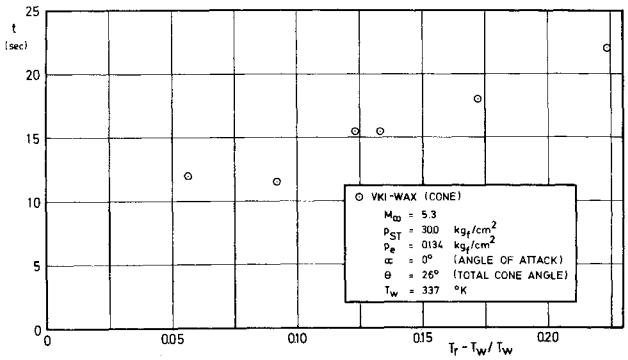

Fig. 3 Run time required for a developed cross-hatched pattern as a function of the driving temperature ratio $(T_r - T_W)/T_W$.

a turbulent recovery factor of 0.895. $T_W = 337$°K is the temperature at which wax liquefies, independent of p_e. Figure 3 shows t as a function of the driving temperature ratio $(T_r - T_W)/T_W$ for a constant static pressure p_e. As may be seen, the run time t is in inverse proportion to the static pressure p_e and increases nearly linearly with the temperature ratio.

3. Expansion Corner

The influence of an expansion wave on the development of cross-hatching has been examined by testing double cone models as sketched in Fig. 4. The result is compared with that on a single cone.

The run was stopped after 15 sec, when a developed pattern appeared on the fore-cone. As may be seen, the pattern on the after-cone has not yet appeared. This is a striking result of the influence of run time. Indeed, the static pressure was lower on the

Received November 19, 1971.

* Research assistant.

† Professor, Brussels University and Head of VKI Department of Supersonics and Hypersonics.